

## Pressure Drops of Water Flow Through Micromachined Particle Filters

Tzung K. Hsiai

Department of Biomedical Engineering and Division of Cardiovascular Medicine, School of Engineering and Keck School of Medicine, Los Angeles, CA 90089-1451. e-mail: hsiai@usc.edu

Sung Kwon Cho and Joon Mo Yang<sup>1</sup>

Mechanical and Aerospace Engineering Department, University of California, Los Angeles, CA 90095

Xing Yang and Yu-Chong Tai

Department of Electrical Engineering, California Institute of Technology, Pasadena, CA 91125

Chih-Ming Ho

Mechanical and Aerospace Engineering Department, University of California, Los Angeles, CA 90095

*When the particle is in the order of microns, flow through the small opening produces a large velocity gradient, leading to high viscous dissipation. Understanding the flow field is critical in determining the power requirement. In this paper, we studied water flow through filters fabricated by micro-electro-mechanical system (MEMS) techniques. The pressure drop calculated by a three-dimensional numerical code of the Navier-Stokes equations is in a reasonable agreement with the experimental data if the diameter and the side wall profile of the holes are measured with high accuracy. [DOI: 10.1115/1.1514209]*

### Introduction

Filtration through thin perforated plates (filters) is a common technique to collect solid particles suspended in fluids, [1]. With the advent of micro electro mechanical system (MEMS) technology, micromachined filters have been designed, [2–4], to isolate biological agents in the order of microns. The filter hole sizes must be less than or comparable to the sizes of target biological agents. Accordingly, the corresponding Reynolds numbers ( $Re_D$ )

are less than 50, much lower than those of conventional filters. The Reynolds number is defined as  $U_{in}D/\beta\nu$ , where  $U_{in}$  is the inlet velocity,  $D$  the hole size,  $\beta$  the opening factor (ratio of area of holes to total area) of the filter, and  $\nu$  the kinematic viscosity of the fluid.  $U_{in}/\beta$  represents the velocity of the fluid passing through the opening.

The empirical formulas established for the conventional filters, [5,6], cannot accurately predict the pressure drop through the microfilters, [4]. Dagan et al. [7] presented an infinite-series solution to the creeping viscous motion of flow through a single hole. Hasegawa et al. [8], who investigated liquid flow through very small orifices (8.8–1000  $\mu\text{m}$ ), demonstrated that the measured pressure drops deviated above those predicted by the Navier-Stokes numerical simulation as the hole size was decreased to micron order.

On the other hand, Yang et al. [9] presented a new design rule to predict the pressure drop of air flow through MEMS filters by embracing the Navier-Stokes numerical simulation with precise geometrical data of the filter. Likewise, we would anticipate good correlation with the Navier-Stokes numerical simulation for water flow through the MEMS filters. It is critical to precisely predict the pressure drop of fluid, which constitutes the basis of biomedical applications. In this context, we studied the pressure drop of water flow through the MEMS based microfilters, and compared the experimental data with the results from three-dimensional Navier-Stokes numerical simulation, [9].

### MEMS Filters

The MEMS filters were fabricated by both surface and bulk micromachining technologies. For details in fabrication processes, please refer to Yang et al. [4], where they showed that the deposition of Parylene C polymer on the surface greatly improves the strength of the MEMS filters. Figure 1 illustrates the MEMS filters by photographs, geometric configuration and the sidewall profiles taken from a scanning electron microscope (SEM). The filtering region was an 8 mm  $\times$  8 mm membrane with a thickness of 3  $\mu\text{m}$ , while the frame region was constructed from a 500- $\mu\text{m}$ -thick silicon wafer. Two filters of different hole sizes (MEMS Filter I and MEMS Filter II, respectively) were fabricated and tested (Table 1).

As shown in Fig. 1(c), sidewalls were not perfectly perpendicular to the surface of the filters. Consequently, the diameters of the front and the back sides were different (Table 1). This variation inevitably occurred as a result of etching processes, [10–12]. Here, the opening factor ( $\beta$ ) was calculated from the hole diameter ( $D$ ) of back side and spacing between the holes ( $s$ ). The precision in measuring the hole diameter of the MEMS filters influenced the accuracy of pressure prediction. A piezo-electrically driven optical interferometer type profiler (WYKO), which provides a lateral resolution of approximately 10 nm (0.01  $\mu\text{m}$ ), was used to profile the surfaces of filters (Fig. 2(a)). Three random locations on each MEMS filter were profiled. Since the hole geometry was not uniformly circular, the diameters were measured in both horizontal and vertical directions. A total of 57

<sup>1</sup>Currently at Nanogen, Inc., San Diego, CA 92121.

Contributed by the Fluids Engineering Division for publication in the JOURNAL OF FLUIDS ENGINEERING. Manuscript received by the Fluids Engineering Division October 19, 2000; revised manuscript received May 16, 2002. Associate Editor: Y. Matsumoto.

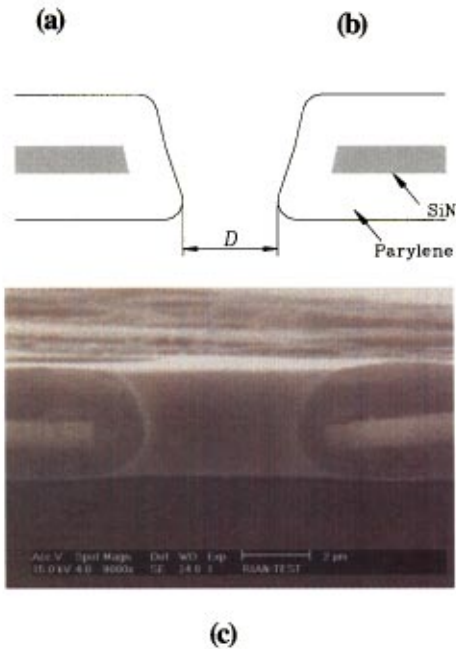
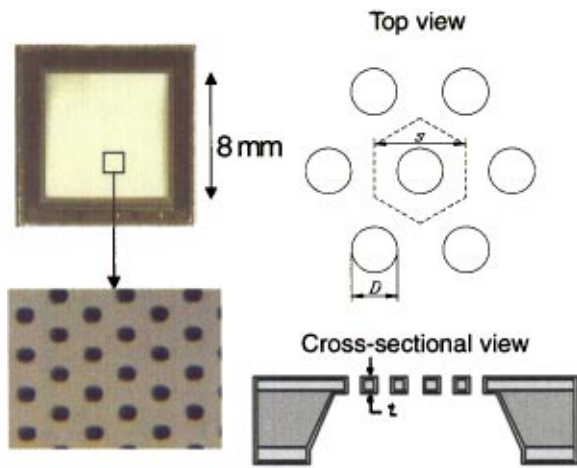


**Fig. 1** Fabricated MEMS Filters with circular holes and thickness of  $3 \mu\text{m}$ : (a) photographs of the MEMS Filter (b) geometric factors in the MEMS Filter (not to scale) (c) side-wall profiles and SEM pictures of the filtering hole

holes were sampled using the WYKO system, from which the probability density functions of the hole diameter and the mean diameters were obtained. Figure 2(b) shows the probability density function of MEMS Filter I. The sidewall geometry of the SEM picture was also profiled, modeled, and incorporated in the three-dimensional Navier-Stokes numerical simulation (see Fig. 1(c)). The measured dimensions of two MEMS filters tested in this experiment are shown in Table 1.

**Table 1** Two MEMS filters (uncertainty in  $D \pm 1\%$  and in  $\beta \pm 2.8\%$ )

Name	Hole Diameter ( $D$ , $\mu\text{m}$ )	Opening Factor ( $\beta$ , %)	Filter Thickness ( $t$ , $\mu\text{m}$ )
MEMS Filter I front side/back side	6.3/6.0	11.2/10.1	3.0
MEMS Filter II front side/back side	7.4/7.2	15.3/14.5	3.0

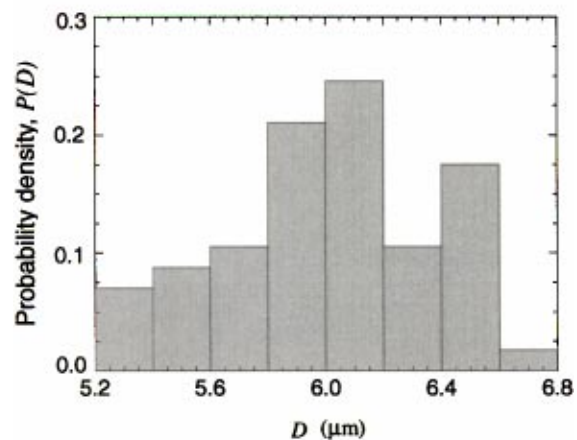
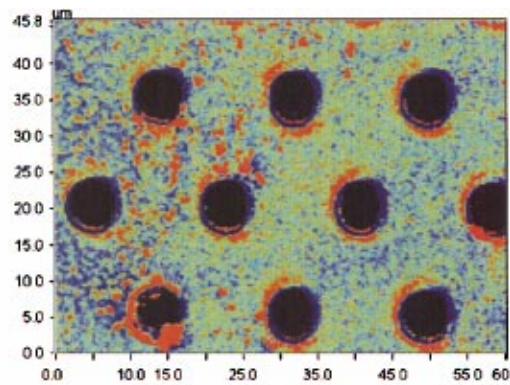


**Fig. 2** (a) Image of the MEMS filtering holes by WYKO surface profiler and (b) probability density function of the hole size for MEMS Filter I (see Table 1)

## Experimental Apparatus

A water channel was designed to measure the pressure drops through the MEMS filters. The water channel was built with an inlet, a settling chamber with sponge and wire mesh, a contraction chamber, and a test channel in which the MEMS filters were positioned. The test channel spanned 16 cm with a cross-section area of  $8 \text{ mm} \times 8 \text{ mm}$  to accommodate the filtering region of the MEMS filters. The contraction contour was derived from a fifth-order polynomial equation to yield an area ratio 3:1. A pressure transducer (Druck LPX 9381, range 0 to 5 psi) was used to measure the static pressure difference between upstream and downstream of the contraction within 0.1% accuracy. By the continuity equation and Bernoulli's principle, we derived the volumetric flow rate, [4,9]. The calculated flow rates validated those obtained from the electromagnetic flow meter (EMCD flow meter, type Mag 1100), which was installed downstream of the test channel. A second pressure transducer, which was connected to two pressure taps at 10 mm upstream and 10 mm downstream from the testing filter, measured the pressure drop through the MEMS filters. The uncertainty in both the pressure and inlet velocity measurement was  $\pm 1.5\%$ . The propagated uncertainties in other physical quantities, which were estimated to be within the 95% confidence level according to Kline et al. [13] and Abernethy et al. [14], are included in the caption of Fig. 3.

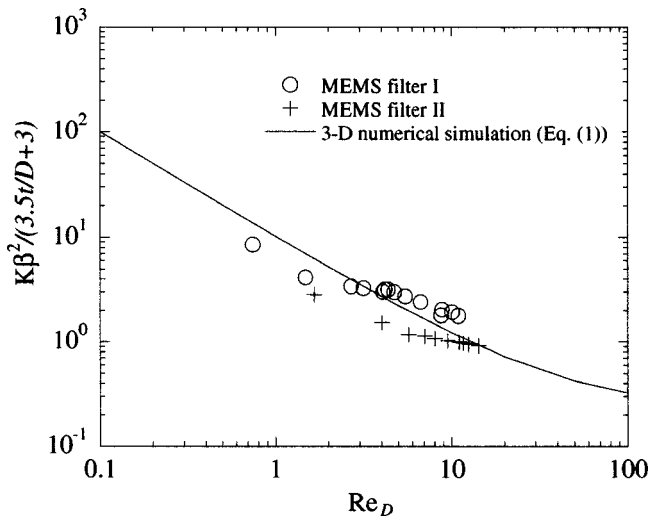


**Fig. 3** The measured pressure drop of MEMS filters in comparison with nondimensionalized numerical formula (Eq. (1)). (Uncertainty in  $K\beta^2/(3.5t/D+3) \pm 6.6\%$  and in  $Re_D \pm 3.3\%$ ).

A constant hydrostatic pressure head was established using a water tank 1.5 meters above the flow channel. The test fluid used was distilled and deionized water (resistivity,  $>4\text{ M}\Omega\text{-cm}$ ). The water was delivered to the tank using a pump (Little Giant Pump Company, model A-430). Purification of the unwanted microparticles was established using two types of filters: (1) water was pumped through a capsule filter (Fisher Scientific, pore size  $0.45\ \mu\text{m}$ ) for two hours prior to experiment and (2) during data collection, water was continuously pumped through a Millipore glass fiber filter (Fisher Scientific, pore size  $0.8\ \mu\text{m}$ ). The flow rate was regulated by a ball valve (McMaster-Carr Supply CO., Nylon miniature ball valve) located upstream from the inlet.

## Results and Discussions

To verify our experimental setup, we compared the pressure drop through conventional screens with Wieghardt's empirical formula, [5]. Our measured pressure drop fell within the acceptable scattering range observed by Wieghardt (not shown). To compare the pressure drops through the MEMS filters, a formula was established using the three-dimensional numerical simulations for laminar water flow at low Reynolds number:

$$K = \frac{\Delta P}{(1/2)\rho U_{in}^2} = \beta^{-2} \left[ 3.1 \frac{t}{D} + 3 \right] \left[ 10.7 \frac{v\beta}{U_{in}D} + 0.22 \right], \quad (1)$$

for  $5\% < \beta < 45\%$ ,  $0.08 < t/D < 0.65$  and  $1 < U_{in}D/\beta v < 100$ , where  $K$  denotes the pressure drop coefficient,  $\Delta P$  the pressure drop through the filters, and  $\rho$  the density of the fluid.

Each individual MEMS filter contained approximately half a million holes of varying sizes. The combination of complex hole geometry and a large number of holes made direct simulation of the entire flow field computationally challenging. Alternatively, we modeled and simulated the averaged geometry of hexagonal domain with a single hole out of the filters. This approach might have been inaccurate. The variation in the diameters of individual holes could have nonlinearly affected the pressure drop according to Eq. (1). Nevertheless, we confirmed that this effect was negligible (less than 2%) by estimating the nonlinear effect of the hole size distribution on the pressure drop using the probability density functions of the hole diameter and Eq. (1). The sidewall profiles, which also influenced the accuracy of the pressure drop prediction, was taken into account in the three dimensional Navier-Stokes numerical simulation. For details in numerical simulations, please refer to Yang et al. [9].

The three-dimensional simulation demonstrated that the pressure drop coefficient varied inversely with the opening factor ( $\beta$ ) to the second power and proportionally with the Reynolds number to the first power. As shown in Fig. 3, the numerical simulation for MEMS filter I overestimated the pressure drop at  $Re_D < 2$ , but underestimated at  $Re_D > 5$ . For the MEMS filter II, the numerical simulation overestimated in the entire testing range of  $Re_D$ . The scattering of the pressure drop may be mainly related to the sensitivity of the numerical simulation to the hole diameter,  $D$ . Despite the installation of two purification filters, impurities could remain from the sponge and wire mesh used to regulate flow upstream. Moreover, the polymer, Parylene C, used to coat the surface of MEMS filters, is known to absorb water over prolonged period of immersion in water.

Nevertheless, the experimental data reasonably agreed with the conventional Navier-Stokes three-dimensional numerical simulation with a maximum of 40% deviation in the range of  $2 < Re_D < 20$ , suggesting that the Navier-Stokes equations in this range of Reynolds number could be applied to model the fluid flow at the micron scale. The characteristic flow scale (the hole size of MEMS filter) was larger than the molecular length scale characterizing the structure of the fluid. Thus, the surface force effect, which might have been dominant in the micron scale, seemed not critical.

## Conclusions

Pressure drops across two MEMS filters with hole sizes of  $6\ \mu\text{m}$  and  $7.2\ \mu\text{m}$ , opening factors of 10.1% and 14.5%, and Reynolds numbers from 20 down to 0.7 were measured and compared with three-dimensional numerical simulation. Geometric factors including precise ratio of hole diameter to filter thickness, sidewall profile, opening factors, and Reynolds number, were taken into account for accurate prediction of the pressure drop. By incorporating the three-dimensional numerical simulation with accurate geometrical data, we were able to reasonably predict the pressure drop through the MEMS filters.

## Acknowledgment

This work was supported by Defense Advanced Research Projects Agency (DARPA) MicroFlumes Program. T. K. H. was supported by National Institutes of Health, NRSA HL # 07895 and UCLA Cardiology Fellowship. The channel could not have become materialized without the technical assistance from John Seymour, Yi-Far Chen, and Eric Prophet. We would also like to thank Dean Ho for conducting the initial testing.

## References

- [1] Ho, C.-M., Huang, P.-H., Yang, J. M., Lee, G.-B., and Tai, Y.-C., 1998, "Active Flow Control by Micro Systems," *FLOWCON*, G. E. A. Meier and P. R. Viswanath, eds., International Union of Theoretical and Applied Mechanics (IUTAM) Symposium on Mechanics of Passive and Active Flow Control, Göttingen, Germany, Kluwer, Dordrecht, The Netherlands, pp. 18–19.
- [2] Kittilsland, G. Steme, G., and Norden, B., 1990, "A Submicron Particle Filter in Silicon," *Sens. Actuators*, **23**, pp. 904–907.
- [3] van Rijn, C. J. M., van der Wekken, M., Hijdam, W., and Elwenpoek, M. C., 1997, "Deflection and Maximum Load of Microfiltration Membrane Sieves Made With Silicon Micromachining," *J. Microelectromech. Syst.*, **6**, pp. 48–54.
- [4] Yang, X., Yang, J. M., Tai, Y. C., and Ho, C.-M., 1999, "Micromachined Membrane Particle Filters," *Sens. Actuators*, **73**(1–2), pp. 184–191.
- [5] Wieghardt, K. E. G., 1953, "On the Resistance of Screens," *Aeronaut. Q.*, **IV**, pp. 186–192.
- [6] Derbunovich, G. I., Zemskaya, A. S., Repik, Ye. U., and Sosedko, Yu. P., 1984, "Hydraulic Drag of Perforated Plates," *Fluid Mech.-Sov. Res.*, **13**(1), pp. 111–116.
- [7] Dagan, Z., Weinbaum, S., and Pfeffer, R., 1982, "An Infinite-Series Solution for the Creeping Motion Through an Orifice of Finite Length," *J. Fluid Mech.*, **115**, pp. 505–523.
- [8] Hasegawa, T., Saganuma, M., and Watanabe, H., 1997, "Anomaly of Excess Pressure Drops of the Flow Through Very Small Orifices," *Phys. Fluids*, **9**, pp. 1–3.
- [9] Yang, J. M., Yang, X., Ho, C. M., and Tai, Y. C., 2001, "Micromachined

Particle filter With Low Power Dissipation," ASME J. Fluids Eng., **123**, pp. 899–908.

- [10] Pelka, J., Weiss, M., Hoppe, W., and Mewes, D., 1989, "The Influence of Ion Scattering on Dry Etch Profiles," J. Vac. Sci. Technol. B, **7**, pp. 1483–1487.
- [11] Daubenspeck, T. H. and Sukanek, P. C., 1990, "Development of Chlorofluorocarbon/Oxygen Reactive Ion Etching Chemistry for Fine-Line Tungsten Patterning," J. Vac. Sci. Technol. B, **8**, pp. 586–595.

[12] May, P. W., Field, D., and Klempere, D. F., 1993, "Simulation of Side-Wall Profiles in Reactive Ion Etching," Journal of Physics D: Applied physics, **26**, pp. 598–606.

[13] Kline, S. J. and McClintock, F. A., 1953, "Describing Uncertainties in Single-Sample Experiments," Mech. Eng. (Am. Soc. Mech. Eng.), **75**, pp. 3–8.

[14] Abernethy, R. B., Benedict, R. P., and Dowdell, R. B., 1985, "ASME Measurement Uncertainty," ASME J. Fluids Eng., **107**, pp. 161–164.